Fusion Science and Technology

ISSN: 1536-1055 (Print) 1943-7641 (Online) Journal homepage: http://ans.tandfonline.com/loi/ufst20

Reducing the Peak-to-Average-Power-Ratio in Fusion Blankets

Marco Riva, Christian Di Sanzo, Mohamed Abdou & Mahmoud Youssef

To cite this article: Marco Riva, Christian Di Sanzo, Mohamed Abdou & Mahmoud Youssef (2017) Reducing the Peak-to-Average-Power-Ratio in Fusion Blankets, Fusion Science and Technology, 72:3, 469-477, DOI: 10.1080/15361055.2017.1333853

To link to this article: https://doi.org/10.1080/15361055.2017.1333853

Published online: 05 Jul 2017.

FUSION SCIENCE AND TECHNOLOGY · VOLUME 72 · 469–477 · OCTOBER 2017

DOI: https://doi.org/10.1080/15361055.2017.1333853

Technical Note

Reducing the Peak-to-Average-Power-Ratio in Fusion Blankets

Marco Riva,* Christian Di Sanzo, Mohamed Abdou, and Mahmoud Youssef

University of California, Fusion Science and Technology Center, Los Angeles, CA 90095

Received September 13, 2016
Accepted for Publication February 28, 2017

Abstract — *Breeding blankets with integrated first wall are one of the most critical components of nuclear fusion reactors. Blankets breeding zones are characterized by steep nuclear heating gradients due to the exothermic nuclear reaction ^{6}Li(n, α)T and the high intensity neutron flux in the proximity of the first wall. Non-uniformity in nuclear heating can generate sharp temperature gradients that deeply affect material properties. This conceptual study explores an original way to flatten nuclear heating profiles by proposing a blanket characterized by layers of different ^{6}Li enrichment in the breeder region while maximizing Tritium Breeding Ratio (TBR) and power generation. Two types of fusion blanket are studied: (1) Helium Cooled Ceramic Reflector (HCCR) and (2) Dual Coolant Lead Lithium (DCLL). For HCCR, it is found in the optimal design case, that the power peak-to-average can be reduced by 47.85%, 42.45% and 54.13% in the front, middle and back channel respectively when compared to the reference design. On the other side, we found that this method of profile flattening is not appealing for DCLL, under the geometrical configuration and material selection in this particular blanket design, since most of nuclear heating is caused by photon heat deposition.*

Keywords — *HCCR, DCLL, breeding reactions, nuclear heating.*

Note — *Some figures may be in color only in the electronic version.*

I. INTRODUCTION

Blankets play a key role in fusion technology by performing power extraction, tritium breeding and shielding. A peculiar characteristic of the fusion environment is the presence of steep nuclear heating gradients that can degrade blanket materials.[1] The neutron flux determines a steep bulk nuclear heating gradient that generates sharp temperature gradients affecting physical properties of materials and generating thermal-mechanical stresses that can compromise performance and integrity of components.[2] In liquid metal blankets, nuclear heating generates buoyancy forces that affect momentum, energy and mass transfer conservation. In particular, in buoyancy-opposed downward flows, mixed convection regime may cause flow reversal and generate inflection points in the velocity profile that becomes potentially unstable.[3]

*E-mail: marco@fusion.ucla.edu

In blanket breeding zones, the nuclear heating is generated by neutrons and photons energy deposition in matter. The main mechanism of neutron heating generation is through the ^{6}Li(n,α)T reaction which releases 4.78 MeV. The typical ^{6}Li enrichment for a Fusion Energy Demonstration Reactor (DEMO) for DCLL and HCCR is 90%. We explore a strategy to flatten nuclear heating deposition, by changing the ^{6}Li concentration in the HCCR and DCLL blankets.

In this preliminary study, the proposed designs are meant to be conceptual, no effort is taken to determine their feasibility, as this is beyond the scope of this study. Particularly, we propose a new concept of blanket in which ^{6}Li enrichment is varied in different blanket channels or within the same channel for solid breeders; these arrangements are considered ideal. The goal of this conceptual neutronics analysis is to determine advantages and disadvantages of this strategy of flattening the nuclear heating gradient. In this preliminary study, we do not consider economics aspects.

II. BLANKETS DESIGN AND MODEL

This study analyzes two Test Blanket Module (TBM) that will be tested in the International Thermonuclear Experimental Reactor (ITER). Neutronics simulations are performed for the Korean HCCR ceramic breeder blanket and the US DCLL liquid metal blanket. MCNP6 1.0 neutron transport code with ENDFB/VII.0 cross section library is used. For convenience, blankets are simulated in a simplified ITER-like wedge reactor model (Fig. 1) with reflective boundary conditions in the azimuthal and z directions and a neutron wall loading (NWL) of 0.78 MW/m^2. The wedge height is equal to the height of the blankets and the wedge wideness is defined by blankets width while radial dimensions and materials are sum up in Table I. Further geometry details are not considered since irrelevant for this conceptual study.

The HCCR is 1670 mm height, 462 mm width and 520 mm thick.[4] It is subdivided into four sub-modules as shown in Fig. 2. The components of each sub-module are: First Wall (FW), Side Wall (SW), Breeding Zone (BZ), Multiplier Zone (MZ), Graphite Reflector (GR). The back of each sub-module is connected to a commune Back Manifold (BM).

The breeder is Li_4SiO_4 and the purge gas is helium. The neutron multiplier is pure beryllium in form of pebbles. The structural material for FW and SW is Advanced Reduced Activation Alloy (ARAA) with helium cooling ducts.

The DCLL consists of a self-cooled eutectic Lead-Lithium (LL) alloy, $Li_{17}Pb_{83}$, for tritium breeding and heat removal at high temperature, and a first wall cooled by helium. LL channels are lined with a Flow Channel Insert (FCI) made of SiC that electrically and thermally insulates channels in order to reduce MHD effects[6] and keep the ferritic structure in the desired temperature window, while LL is maintained at high temperature to optimize power conversion. The components of DCLL are: FW with Be coating, LL channels, structure (F82H), FCI (SiC), Inner/Outer Helium manifolds and back plate. The blanket is 1660 mm height, 484 mm width and 352 mm thick.[7] However, we simulate only the mid-plane section (1275 mm height) which represents 77% of TBM as shown in Fig. 3. Note that the front and back channels are respectively subdivided into three sub-channels (F1, F2, F3 and B1, B2, B3).

The FW is modeled as three layers in both blankets: FW front channel (100% F82H), cooling channel (83% He, 17% F82H), back plate (100% F82H).

TABLE I

ITER-Like Model Material Compositions and Dimensions

Component	Radial Thickness [cm]	Material	% Volume
Magnet	87.5	SS316 Epoxy Cu Nb_3Sn He Liquid Bronze	47% 13.3% 12% 3% 17.2% 7.5%
Gap	16	Void	–
Shield	33.5	SS316 H_2O	75% 25%
Gap	3	Void	–
Shield	33.5	SS316 H_2O	75% 25%
FW	2	Cu H_2O SS316	70% 20% 10%
FW coating SOL Plasma SOL	1 14 400 24.8	Be Void Void Void	100% – – –
BLANKET+FW: HCCR DCLL	 52 32.5		
Shield	33.5	SS316 H_2O	75% 25%

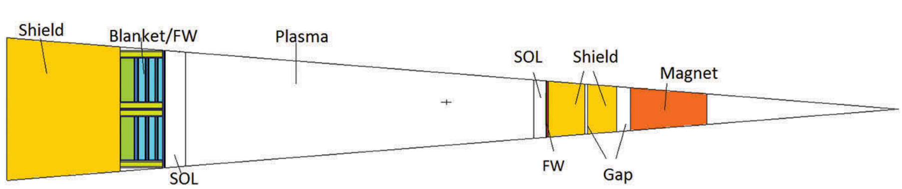

Fig. 1. MCNP ITER-like reactor wedge model.

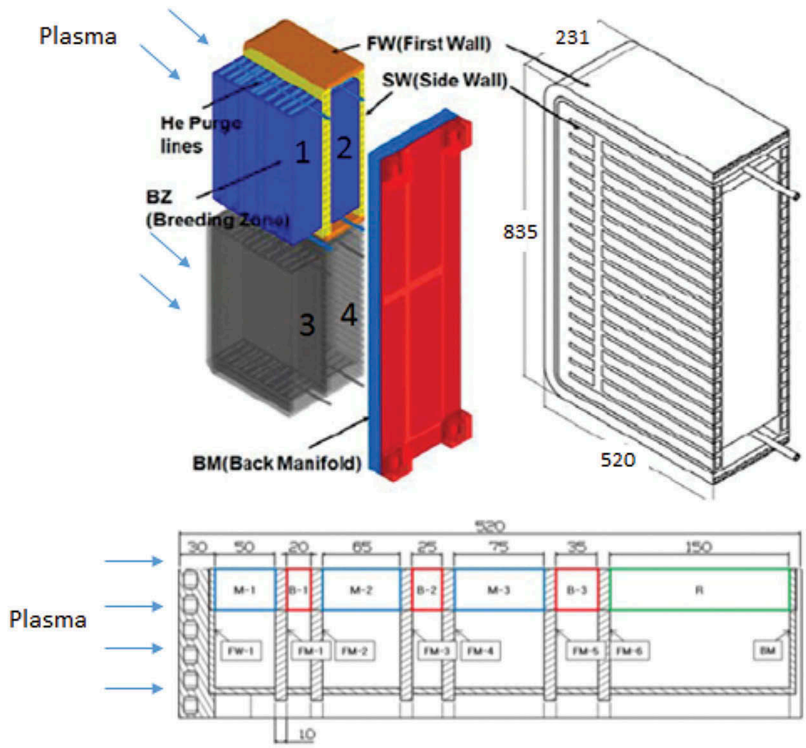

Fig. 2. KO HCCR TBM and its sub-modules.[5] The numbers in the figure indicate each HCCR sub-module. (Edited by Ref. 5).

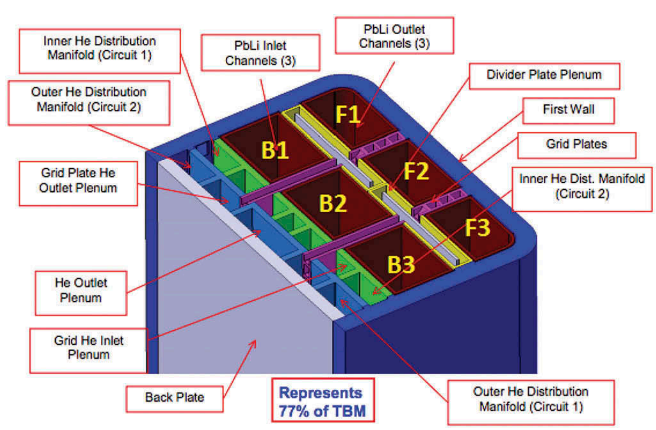

Fig. 3. Configuration at mid-plane of TBM. (Edited by Ref. 6).

III. RESULTS

III.A. Helium Cooled Ceramic Reflector—HCCR

Neutronics simulations have been performed for the HCCR breeding blanket. The reference design has 90% enrichment in ^{6}Li and uses lithium orthosilicate pebbles with 0.64 packing fraction. A considerable part of the neutron current passing through the FW is at lower energy than 14.58 MeV because of neutron back-scattering in the inboard region of the reactor.

The local TBR in the whole blanket (four sub-modules) is 0.95 for a total tritium production rate of 1.27×10^{-6} g/s. The total nuclear heating in the TBM is 0.672 MW. Nuclear heating gradient in sub-module 1 (Fig. 2) is shown in Fig. 4. It is found that the most of the nuclear heating is due to neutrons energy deposition while photons contribution is negligible. 2-D plots of nuclear heating are shown in Fig. 5.

Reducing ^{6}Li enrichment of pebbles close to the multiplier zones, where the neutron flux is higher, would decrease nuclear heating peaks and flatten the nuclear heating profile. Four designs (A, B, C, D) are considered. In all designs the breeding zone ^{6}Li enrichment is varied from a minimum value at the border to a maximum value in the center of the channel, in a way to counter the nuclear heating profile. To vary the enrichment, the pebble bed breeding zones are divided into multiple sub-layers of 0.5 mm; ^{6}Li enrichments in each sub-layer for designs A, B, C and D are summarized in Table II. Our simulations have shown that 0.5 mm sub-layer thickness is necessary to obtain a continuous flat profile. The feasibility of such a design is not the goal of this technical note and, therefore, it is not discussed. However, much effort has been made by the fission community to arrange pebbles with different uranium enrichment in specific core regions of Advanced High

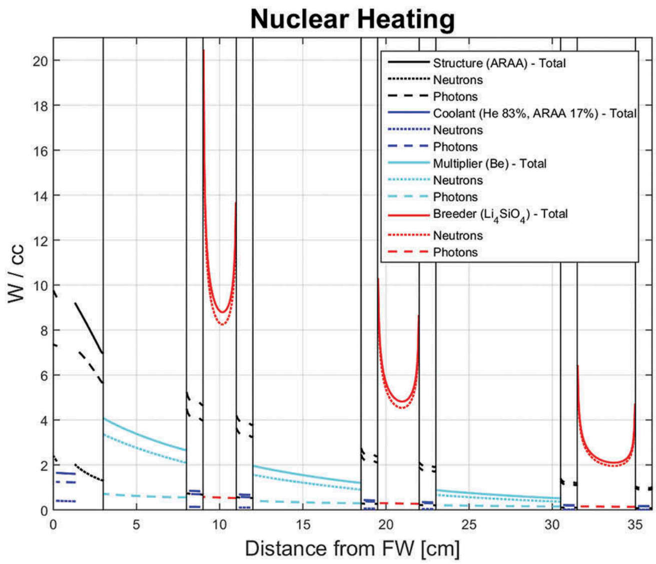

Fig. 4. Radial nuclear heating deposition for sub-module 1 of HCCR in the reference design (90% ^{6}Li enrichment). Graphite reflector is not shown.

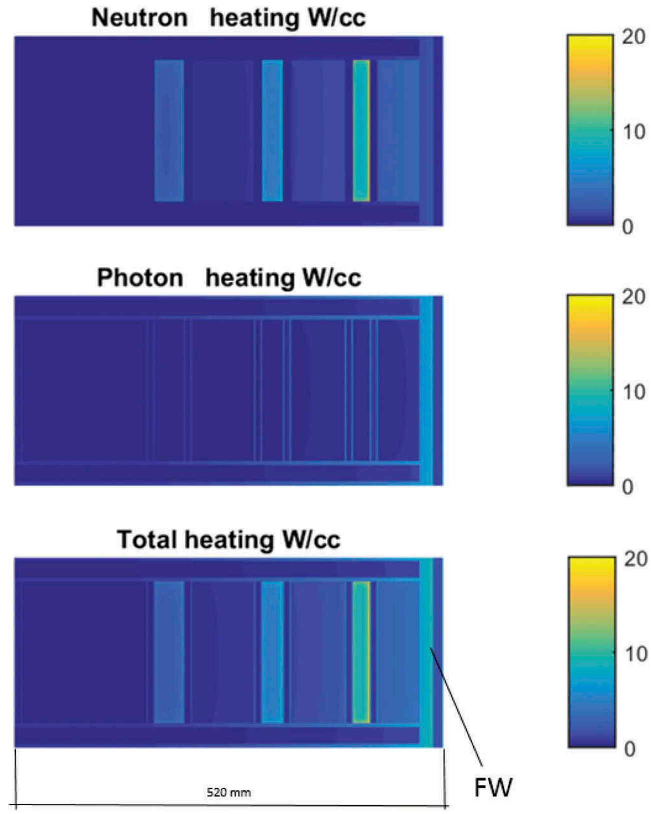

Fig. 5. Nuclear heating deposition for sub-module 1 of HCCR in the reference design (90% ^{6}Li enrichment).

Temperature Reactors (AHTR) and the topic is still under study. In particular, *Peterson et al.* have performed experiments to fill out a reproduction of a Modular Pebble-Bed AHTR reactor core in a multi-layer configuration.[8] Moreover, in Ref. 2 it is shown, throughout Discrete Element Method (DEM) simulations, that only pebble fragments of broken pebbles can travel within the bed. Pebble beds are tightly packed structures and pebble relocation during heating is negligible. An exception is during fragmentation due to pebble crushing. However, even up to 10% of pebbles in an ensemble crushing, the effects on neutronics due to rearrangement is negligible.

The nuclear heating profiles in the front channel for various designs are presented in Fig. 6. Middle and back channel have qualitatively similar profiles. Peak-to-Average-Power-Ratio (PAPR), Heat Deposition (HD), TBR, and their reduction with respect to the reference design for sub-module 1 of the HCCR (Fig. 2), are summarized in Table III with their respective statistical error.

PAPR reduction is maximized in designs A and B (~46%, ~42%, ~54% respectively in the front, middle and back channel). The contribution of ^{7}Li (n, n', α)T to TBR is increased because of the higher concentration of ^{7}Li while a more thermalized neutron flux allows a higher ^{6}Li(n, α)T reaction cross section. The total effect is a relatively low decrease of power deposition and TBR. The optimal design is found to be design A that has a >45% PAPR reduction and a small decrease in power deposition (1.82%) and TBR (1.92%).

III.B. Dual Coolant Lead Lithium—DCLL

Neutronics simulations of the DCLL breeding blanket reference design (90% ^{6}Li) give a local TBR of 0.555 and a tritium production rate of 5.92×10^{-7} g/s in good agreement with Ref. 6. In the front channel, 59.7% of nuclear heating is generated by photons energy deposition while neutrons play a marginal role in defining the nuclear heating gradient shape as shown in Fig. 7. Such a high gamma production is due to the inelastic scattering in lead, typical of heavy elements. We simulated three alternative designs; a two-channel design A (7.5%, 90% ^{6}Li in front and back channels respectively) and two four-channel designs, B and C. For designs B and C, each channel of Fig. 3 is split into two sub-channels in the direction parallel to the first wall. The two sub-channels are separated by FCI and structure. We compare the heat deposition of these designs in Fig. 8. Table IV summarizes PAPR, HD, TBR and ^{6}Li enrichment for channels F2 and B2 (Fig. 3) reference design and design A, as well as for the two four-channel designs B and C. In Table IV, the results of the new front and back sub-channels of design B and C are averaged and compared to the respective original channel of the reference design.

TABLE II

^{6}Li Enrichment in Sub-Layers for Designs A, B, C, D in the Front Channel

Front Channel	^{6}Li Enrichment %				Middle Channel	^{6}Li Enrichment %				Back Channel	^{6}Li Enrichment %			
Sub-Layer #	A	B	C	D	Sub-Layer #	A	B	C	D	Sub-Layer #	A	B	C	D
1	37.5	32.5	50	42.5	1	42.5	37.5	57.5	50	1	30	27.5	50	50
2	45	40	62.5	52.5	2	50	45	67.5	57.5	2	35	32.5	62.5	57.5
3	52.5	47.5	72.5	62.5	3	55	50	75	65	3	40	37.5	72.5	65
4	60	52.5	80	70	4	60	55	80	70	4	45	42.5	80	70
5	65	57.5	85	75	5	65	57.5	85	75	5	50	47.5	85	75
6	70	62.5	90	80	6	70	60	90	77.5	6	55	50	90	77.5
7	75	67.5	92.5	82.5	7	72.5	62.5	92.5	80	7	57.5	52.5	92.5	80
8	77.5	70	95	85	8	75	65	95	82.5	8	60	55	95	82.5
9	80	72.5	95	85	9	77.5	67.5	95	85	9	65	57.5	95	85
10	82.5	75	95	85	10	80	70	95	85	10	67.5	60	95	85
11	85	77.5	95	85	11	82.5	72.5	95	85	11	70	62.5	95	85
12	87.5	80	95	85	12	85	75	95	85	12	72.5	65	95	85
13	90	82.5	95	85	13	87.5	77.5	95	85	13	75	67.5	95	85
14	92.5	85	95	85	14	90	80	95	85	14	77.5	70	95	85
15	95	8.75	95	85	15	92.5	82.5	95	85	15	80	72.5	95	85
16–32	95	90	95	85	16	95	85	95	85	16	82.5	75	95	85
33	95	87.5	95	85	17	95	87.5	95	85	17	85	77.5	95	85
34	92.5	85	95	85	18–38	95	90	95	85	18	87.5	80	95	85
35	90	825	95	85	39	95	87.5	95	85	19	90	82.5	95	85
36	87.5	80	92.5	82.5	40	92.5	85	95	85	20	92.5	85	95	85
37	85	77.5	92.5	82.5	41	90	82.5	95	85	21	95	87.5	95	85
38	80	72.5	90	80	42	87.5	80	95	85	22–57	95	90	95	85
39	72.5	65	82.5	72.5	43	85	77.5	95	85	58	95	87.5	95	85
40	62.5	55	70	62.5	44	82.5	75	95	85	59	95	85	95	85
–	–	–	–	–	45	80	72.5	95	82.5	60	92.5	82.5	95	85
–	–	–	–	–	46	77.5	70	95	80	61	90	80	95	85
–	–	–	–	–	47	72.5	65	90	77.5	62	87.5	77.5	95	85
–	–	–	–	–	48	67.5	60	87.5	72.5	63	85	75	95	85
–	–	–	–	–	49	60	52.5	80	65	64	82.5	70	95	85
–	–	–	–	–	50	50	45	67.5	55	65	80	65	95	82.5
–	–	–	–	–	–	–	–	–	–	66	77.5	60	92.5	80
–	–	–	–	–	–	–	–	–	–	67	72.5	55	92.5	77.5
–	–	–	–	–	–	–	–	–	–	68	67.5	50	90	72.5
–	–	–	–	–	–	–	–	–	–	69	60	42.5	82.5	65
–	–	–	–	–	–	–	–	–	–	70	52.5	35	70	55

It is seen that photon heating of design A and reference case are very similar. In the front channel of design A, the photon heating is slightly higher because of increased gamma production from ^{7}Li (present at 92.5%). On the other hand, the total heating is lower since neutron power deposition is reduced. In the back channel the total heating is higher because of the higher ^{6}Li(n, α)T reaction rate caused by a more thermalized flux. However, there is no PAPR reduction while HD and TBR decrease from 71.63 kW and 0.185 to 66.3 kW 0.137 in the central zone of design A (channels F2 and B2).

Averaging the two front and two back channels of the four-channel designs, B and C, we obtain a PAPR reduction of 20.12% and 15.29% for designs B and C front channel due to a higher average volumetric heat deposition in every sub-channel. However, these two designs show high HD and TBR reduction (above 24% and 44% respectively in the front channel) because of the lower amount of breeder, due to the space occupied by the new channel separator.

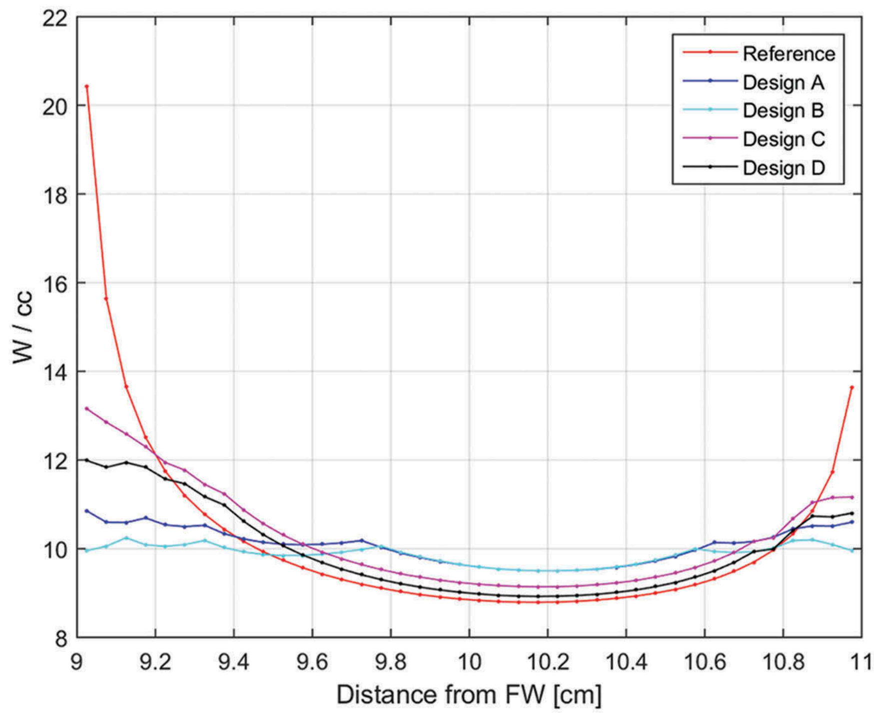

Fig. 6. Nuclear heating in the front channel for the designs A, B, C, D and reference design.

TABLE III

Peak-to-Average-Power-Ratio, Heat Deposition and TBR Decrease for Designs A, B, C, D Compared to the Reference Design for HCCR*

Design	PAPR	Statistical Error	Difference	HD [kW]	Statistical Error	Difference	TBR	Statistical Error	Difference
Front Channel									
Reference	1.99	0.11%	–	27.19	0.09%	–	0.109	0.10%	–
A	1.08	0.11%	–45.86%	26.70	0.09%	–1.82%	0.107	0.10%	–1.92%
B	1.04	0.11%	–47.85%	26.17	0.09%	–3.76%	0.105	0.10%	–3.94%
C	1.28	0.11%	–35.62%	27.20	0.09%	0.01%	0.109	0.10%	0.00%
D	1.20	0.11%	–39.53%	26.39	0.09%	–2.95%	0.106	0.10%	–3.12%
Middle Channel									
Reference	1.82	0.16%	–	18.65	0.10%	–	0.078	0.11%	–
A	1.07	0.16%	–41.47%	18.41	0.10%	–1.30%	0.077	0.11%	–1.67%
B	1.05	0.16%	–42.45%	18.12	0.11%	–2.83%	0.076	0.12%	–3.21%
C	1.27	0.16%	–30.24%	18.70	0.10%	0.26%	0.078	0.12%	0.26%
D	1.24	0.16%	–32.23%	18.30	0.11%	–1.90%	0.076	0.12%	–1.93%
Back Channel									
Reference	2.47	0.25%	–	12.00	0.14%	–	0.051	0.15%	–
A	1.12	0.25%	–54.60%	11.80	0.14%	–1.63%	0.050	0.14%	–2.55%
B	1.13	0.26%	–54.13%	11.68	0.13%	–2.63%	0.049	0.14%	–3.53%
C	1.54	0.24%	–37.77%	12.06	0.15%	0.49%	0.051	0.13%	0.59%
D	1.47	0.25%	–40.69%	11.86	0.14%	–1.13%	0.050	0.15%	–1.19%

*Results refer only tp sub-module 1 of Fig. 2.

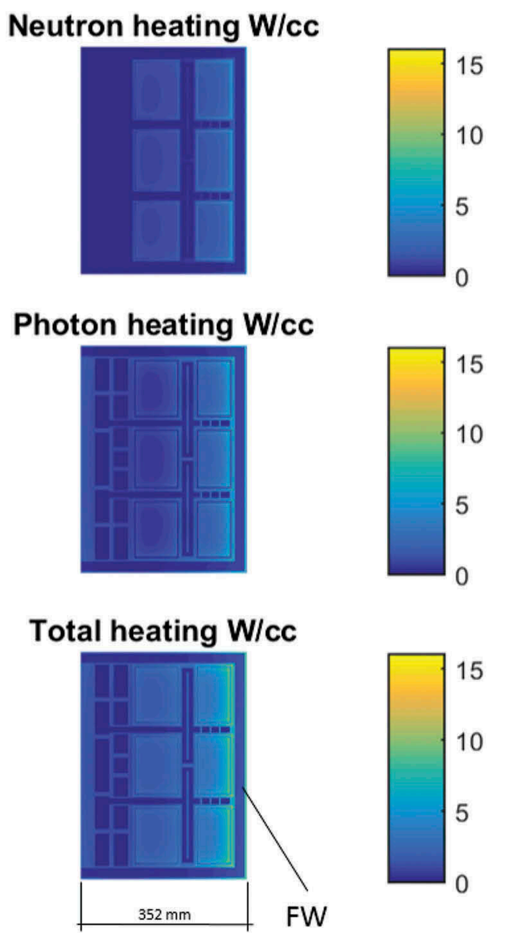

Fig. 7. Nuclear heating deposition in the DCLL breeding blanket for reference design (90% ^{6}Li enrichment).

IV. CONCLUSIONS

We presented a strategy to minimize the Peak-to-Average-Power-Ratio nuclear heating and reduce the spatial dependence of heat deposition in HCCR and DCLL blankets by controlling ^{6}Li enrichment. A multi-layer conceptual design was introduced for HCCR. It was found that PAPR of front, middle and back channel of the HCCR is reduced by 45.86%, 41.47% and 54.60% (design A). Reductions in TBR and total power deposition are minimized due to an increased ^{6}Li(n, α) microscopic cross section. Further studies will be performed on DEMO ceramic blanket designs to understand if a TBR of ~1.1 can be reached when the enrichment is reduced in the channels that are closer to the FW, where the PAPR is generally higher because of the very hard neutron flux. To improve the design feasibility a unique enrichment in each channel can be considered.

It was found that nuclear heating in DCLL blankets is related to photons heat deposition in lead. For this reason, designing the DCLL as a multi-channel blanket with different ^{6}Li enrichments in different channels have minimum effect on nuclear heating gradient shape. However, a reduction in PAPR is found for four-channel designs, though at the expense of a drastic reduction in TBR and total heat deposition. Further studies are needed to minimize photon

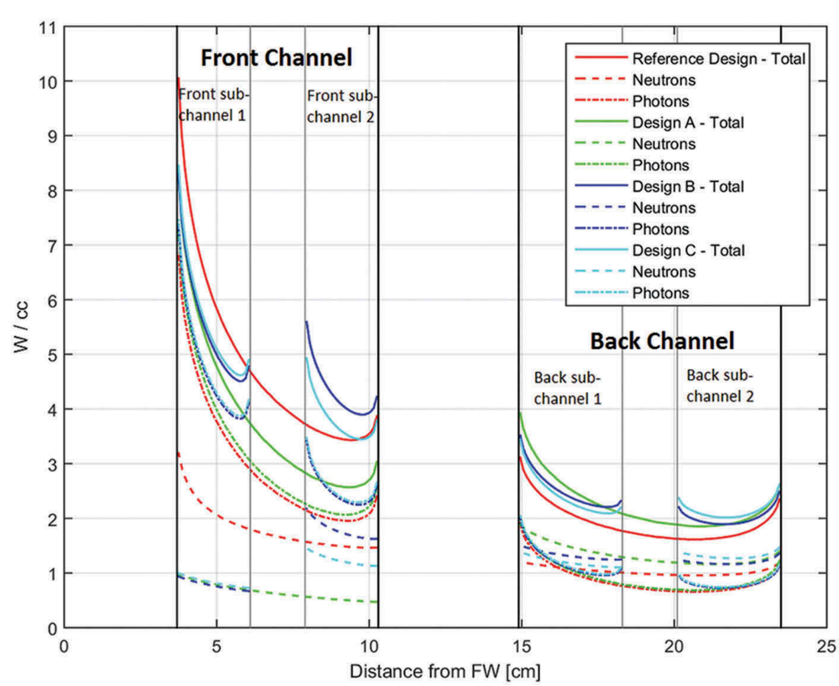

Fig. 8. Radial profiles of nuclear heating in DCLL for Reference, A, B, and C designs.

TABLE IV

Peak-to-Average-Power-Ratio, Heat Deposition and TBR Difference for Designs A, B, C Compared to Reference Design for DCLL and Their Respective Statistical Error*

	Front Channel			Back Channel		
	PAPR	HD [kW]	TBR	PAPR	HD [kW]	TBR
Reference	^{6}Li 90%			^{6}Li 90%		
	2.12	46.99	0.105	1.64	24.64	0.080
Statistical error	0.08%	0.10%	0.11%	0.08%	0.10%	0.10%
Design A	^{6}Li 7.5%			^{6}Li 90%		
	2.21	37.21	0.030	1.75	29.09	0.107
Statistical error	0.08%	0.11%	0.11%	0.08%	0.11%	0.10%
Difference	3.97%	–20.82%	–71%	6.71%	18.04%	34%

	Front Sub-Channel 1			Front Sub-Channel 2			Back Sub-Channel 1			Back Sub-Channel 2		
	PAPR	HD [kW]	TBR	PAPR	HD [kW]	TBR	PAPR	HD [kW]	TBR	PAPR	HD [kW]	TBR
Design B	^{6}Li 7.5%			^{6}Li 60%			^{6}Li 80%			^{6}Li 90%		
	1.51	19.79	0.015	1.30	15.53	0.044	1.39	12.89	0.045	1.24	10.29	0.043
Statistical error	0.08%	0.10%	0.15%	0.08%	0.10%	0.11%	0.9%	0.09%	0.10%	0.08%	0.10%	0.11%
Average	1.70		35.32		0.059		1.75		23.17		0.088	
Difference	–20.12%		–24.83%		–44%		6.71%		–5.96%		10%	
Design C	^{6}Li 7.5%			^{6}Li 30%			^{6}Li 60%			^{6}Li 90%		
	1.51	20.21	0.016	1.30	13.71	0.030	1.43	12.36	0.040	1.22	10.95	0.048
Statistical error	0.08%	0.10%	0.15%	0.08%	0.11%	0.11%	0.9%	0.09%	0.11%	0.09%	0.10%	0.11%
Average	1.80		33.92		0.046		1.61		23.32		0.088	
Difference	–15.29%		–27.81%		–57%		–1.63%		–5.38%		10%	

*For designs B and C, "average" means an average of the two front and the two back sub-channels to allow a comparison with the reference front and back channels.

heat deposition and optimize total heat deposition and TBR.

ORCID

Marco Riva http://orcid.org/0000-0001-7262-0688

References

1. M. ABDOU et al., "Blanket/First Wall Challenges and Required R&D on the Pathway to DEMO," *Fusion Eng. Des.*, **100**, 2 (2015); https://doi.org/10.1016/j.fusengdes.2015.07.021.

2. J. T. VAN LEW et al., "Numerical Study on Influences of Bed Resettling, Breeding Zone Orientation, and Purge Gas

on Temperatures in Solid Breeders," *Fusion Eng. Des.*, in press (2016).

3. S. SMOLENTSEV et al., "Dual-Coolant Lead-Lithium (DCLL) Blanket Status and R&D Needs," *Fusion Eng. Des.*, **100**, 44 (2015); https://doi.org/10.1016/j.fusengdes.2014.12.031.

4. S. CHO et al., "Overview of Helium Cooled Ceramic Reflector Test Blanket Module Development in Korea," *Fusion Eng. Des.*, **88**, *6*, 621 (2012); https://doi.org/10.1016/j.fusengdes.2013.05.072.

5. D. WON LEE et al., "Functional Components Design and Analysis of a Korean HCCR TBM in ITER," *IEEE 25th Symp. on Fusion Engineering (SOFE)*, San Francisco, California, June 10–14, 2013; https://doi.org/10.1109/SOFE.2013.6635374.

6. S. SMOLENTSEV et al., "Magnetohydrodynamic and Thermal Issues of the SiCf/SiC Flow Channel Insert," *Fusion Sci. Technol.*, **50**, *1*, 107 (2006); https://doi.org/10/13182/FST06-A1226.

7. M. E. SAWAN et al., "Neutronics Performance Parameters for the U.S. Dual Coolant Lead Lithium ITER Test Blanket Module," *23rd IEEE/NPSS Symp. on Fusion Engineering (SOFE)*, San Diego, California, May 31–June 5, 2009; https://doi.org/10.1109/FUSION.2009.5226451.

8. P. F. PETERSON, *Modular Pebble-Bed AHTR Design Review*, University of California, Berkeley (Oct. 7, 2009).